Andean Geology 38 (1): 64-81. January, 2011

Andean Geology
formerly Revista Geológica de Chile
www.scielo.cl/andgeol.htm

Magnetic fabric and microstructures across the Andes of Tierra del Fuego, Argentina

Federico Esteban[1], Alejandro Tassone[1], Marco Menichetti[2], Augusto E. Rapalini[1], Marcela B. Remesal[3], María Elena Cerredo[3], Horacio Lippai[1], Juan F. Vilas[1]

[1] *CONICET-INGEODAV, Departamento de Ciencias Geológicas, Facultad de Ciencias Exactas y Naturales, Universidad de Buenos Aires, Ciudad Universitaria, Pabellón 2, C1428EHA Ciudad Autónoma de Buenos Aires, Argentina.*
esteban@gl.fcen.uba.ar; atassone@gl.fcen.uba.ar; rapalini@gl.fcen.uba.ar; lippai@gl.fcen.uba.ar; vilas@gl.fcen.uba.ar

[2] *Istituto di Scienze della Terra, Università di Urbino, Campus Scientífico Universitario, 61029 Urbino,Italy.*
marco.menichetti@uniurb.it

[3] *CONICET-Departamento de Ciencias Geológicas, Facultad de Ciencias Exactas y Naturales, Universidad de Buenos Aires, Ciudad Universitaria, Pabellón 2, C1428EHA Ciudad Autónoma de Buenos Aires Argentina*
remesal@gl.fcen.uba.ar; cerredo@gl.fcen.uba.ar

ABSTRACT. An anisotropy of magnetic susceptibility (AMS) transect was carried out across the Fuegian Andes, in Argentina, with the aim of studying its tectonic evolution. Two-hundred and forty oriented samples were collected from 27 sites distributed between the Paso Garibaldi to the north and the Canal Beagle to the south. The study was restricted to the Upper Jurassic Lemaire Formation, with a single site located in the Lower Cretaceous Yahgán Formation. Studied rocks comprised basaltic, andesitic, volcaniclastic and sedimentary rocks affected by low-grade metamorphism. AMS measurements were complemented with thin section analyses of representative samples in order to characterize the microstructures and metamorphic assemblages. In general, the magnetic fabric shows dominant oblate shapes and a large variation in the anisotropy degree from 1.04 up to 2. The anomalously high values were observed to be associated to growth of secondary pyrrhotite, which was identified by rock magnetic tests. Magnetic foliation was generally consistent with slaty cleaveage as observed in the field, confirming the tectonic origin of the magnetic fabric. Three geographic domains were distinguished in the study region on the basis of the pattern of the AMS axes distribution. In the northern domain, from Paso Garibaldi to Valle Carbajal, the orientation of the maximum susceptibility axis (κ_1), or magnetic lineation, is N-S to NE-SW with moderate plunge towards the S-SW and coincides with previous determination of mineral lineations associated with the Andean deformation and very low grade metamorphism. The magnetic fabric pattern can be correlated with the main deformational phase responsible for the development of slaty cleavage (main Andean deformational phase) and the tectonic transport due to progression of the Fuegian fold and thrust belt in the Late Cretaceous. A different character is shown along the Valle Carbajal domain, where subvertical E-W magnetic foliation planes and roughly E-W to ESE-WNW subhorizontal magnetic lineations are more difficult to correlate with the main folding phase and suggest its relation to an E-W, possibly localized, strike-slip regime during the main deformational and metamorphic phase. The magnetic fabrics in the third domain, close to the Canal Beagle, displays a more heterogeneous character with both E-W and N-S striking foliations; in this case a population of subhorizontal E-W magnetic lineation (κ_1) suggests the existence of a significant component of strike-slip deformation.

Keywords: AMS, Microstructures, Mesozoic, Andean tectonics, Tierra del Fuego, Argentina.

RESUMEN. Fábrica Magnética y Microestructuras a través de los Andes de Tierra del Fuego, Argentina. Se presentan los resultados de una transecta de Anisotropía de Susceptibilidad Magnética (ASM) realizada en los Andes Fueguinos, Argentina. Se midieron 240 muestras orientadas provenientes de 27 sitios de muestreo distribuidos entre Paso Garibaldi, al norte y el Canal Beagle al sur. El muestreo se focalizó esencialmente en la Formación Lemaire del Jurásico Superior, con un único sitio en la Formación Yahgán del Cretácico inferior. Las litologías estudiadas incluyen basaltos, andesitas y rocas volcanoclásticas y sedimentarias afectadas por metamorfismo de bajo grado. Las mediciones de fábrica magnética se complementaron con el estudio microscópico de muestras representativas con el propósito de caracterizar las microestructuras y las asociaciones metamórficas. La fábrica magnética está dominada por formas obladas y presenta una gran variación en el grado de anisotropía (1,04-2). Los mayores valores de anisotropía están asociados a la presencia de pirrotina secundaria, identificada por medio de ensayos magnéticos. La foliación magnética muestra muy buena correspondencia con el clivaje medido en campo, confirmando el origen tectónico de la fábrica magnética. Los modelos de distribución de los ejes de ASM permitieron distinguir tres dominios geográficos. El dominio septentrional, entre Paso Garibaldi y Valle Carbajal, presenta lineaciones magnéticas (k1) de orientación N-S a NE-SW con buzamiento moderado hacia el S-SW, coincidente con determinaciones previas de lineaciones minerales asociadas con la deformación andina. Este diseño de fábrica magnética se vincula a la fase de deformación principal responsable del desarrollo del clivaje pizarreño y de la faja plegada y corrida Fueguina en el Cretácico Tardío. Un segundo dominio corresponde al Valle Carbajal, caracterizado por foliaciones magnéticas E-W, subverticales y lineaciones magnéticas E-W (a ESE-WNW) subhorizontales que se interpretan como vinculados a regímenes localizados de transcurrencia. La fábrica magnética en el tercer dominio, en la zona del Canal Beagle, presenta un carácter más heterogéneo con foliaciones de orientación tanto E-W como N-S; la presencia de una población de lineaciones magnéticas subhorizontales de rumbo E-W sugiere la existencia de un componente de rumbo significativo.

Palabras clave: ASM, Microestructuras, Mesozoico, Tectónica andina, Tierra del Fuego, Argentina.

1. Introduction

Magnetic fabric and microstructural studies in orogenic belts provide significant information regarding the type and degree of tectonic deformation affecting the main lithologic units exposed along them (Tarling and Hrouda, 1993; Borradaile and Henry, 1997). Despite its resolution, versatility and speed, magnetic fabric studies in orogenic belts are scarce in South America and particularly in the Southern Andes (Rapalini *et al.,* 2005a and b; Zaffarana *et al.,* 2008). As part of a long-term and interdisciplinary project to study the tectonic evolution of the Fuegian Andes, a magnetic fabric transect across the Andean chain in the Argentine side of the Tierra del Fuego island (Figs. 1 and 2) was carried out.

The region of Tierra del Fuego can be subdivided in at least three physiographic provinces (Fig. 1) with the main chain corresponding with the Late Cretaceous orogen of the Fuegian Cordillera in the SW where a thick-skinned tectonic style prevails. Northward the basement's sole thrusts crop out in the Magallanes fold-and-thrust belt where a thin-skinned tectonic style dominates, which progrades to the scarcely deformed foreland. The main Cordillera and the Magallanes fold-and-thrust belt are affected by a strike-slip fault system. Wrench tectonics affected the region during the Andean compressional phase and especially from the Oligocene onwards (*e.g.,* Bruhn, 1979; Klepeis, 1994; Cunningham, 1995; Diraison *et al.,* 2000; Lodolo *et al.,* 2001; Menichetti *et al.,* 2008 and references therein).

Our work was concerned with an area located within the Fuegian Cordillera in central Tierra del Fuego (Fig. 1). The scope was the study of the magnetic fabric jointly with petrographic and structural analyses in order to provide additional information regarding the tectonic evolution of this orogenic region. Since this has had a complex geologic evolution a multidisciplinary approach is considered the most suitable.

2. Geological Framework of the southernmost Andes

The geology of Tierra del Fuego shows a complex tectonic evolution since the late Paleozoic. A major tectonic event was the widespread extensional regime in the Late Jurassic that led to formation of the Rocas Verdes marginal basin (RVB) along the southern Patagonian and Fuegian continental margin (Dalziel *et al.,* 1974; Suárez and Pettigrew, 1976; Hanson and Wilson, 1991; Calderón *et al.,* 2007). In the Late Cretaceous, compression in the Pacific margin of the South American plate led to the closure and inversion of the basin and the development of the Andean orogen with its associated fold-and-thrust

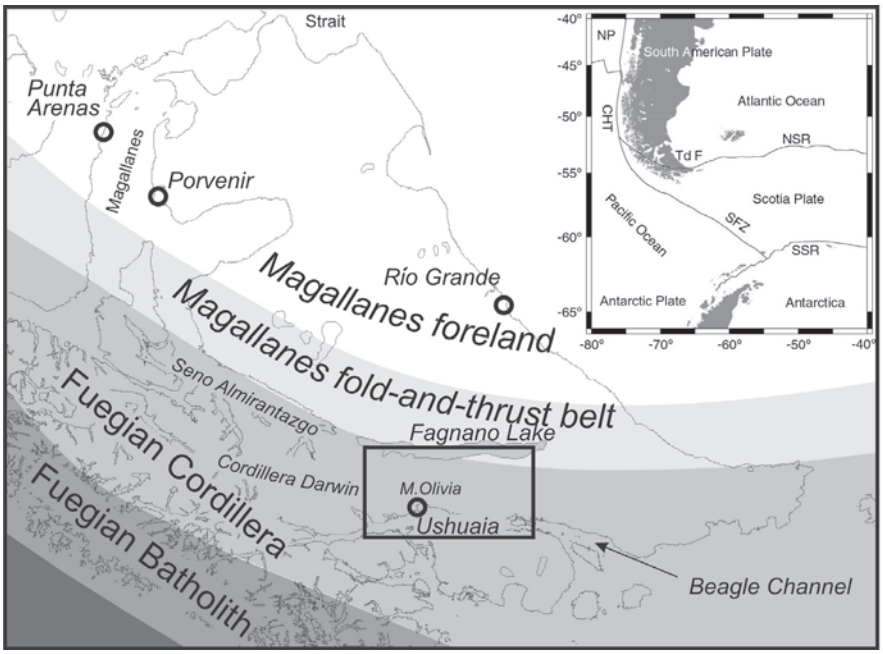

FIG. 1. Map depicting the main morphostructural provinces in Tierra del Fuego; box indicates the area of figure 2. Inset shows the major plates and plate boundaries-Nazca plate (NP), Chile trench (CHT), North Scotia Ridge (NSR), Shackleton Fracture Zone (SFZ), Tierra del Fuego (TdF) setting.

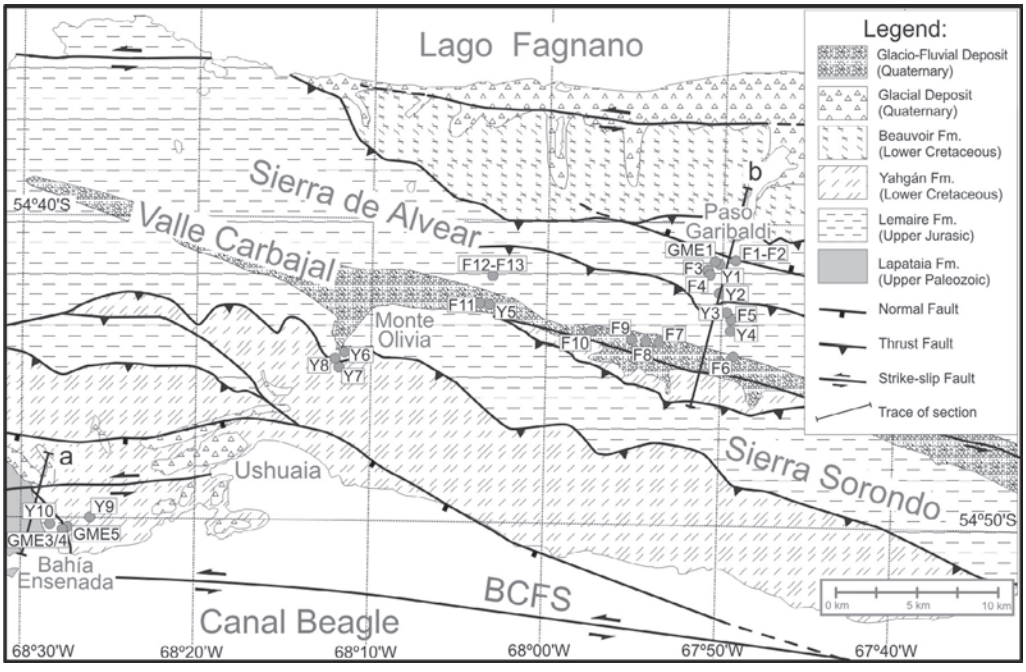

FIG. 2. Schematic geological map across Sierra Alvear and Sierra Sorondo in the southern part of the Tierra del Fuego Island from Ushuaia to Lago Fagnano (after Olivero Martinioni, 2008; Peroni *et al.,* 2009). Location of the AMS sampling sites are indicated in the square boxes. The trace of the sections a and b are referred respectively to the figures 3 and 4. **BCFS:** Beagle Channel Fault System.

belt (Dalziel *et al.,* 1974; Wilson, 1991; Bruhn, 1979; Nelson *et al.,* 1980; Diraison *et al.,* 2000; Kraemer, 2003; Menichetti *et al.,* 2008). Since the Paleocene, in correspondence with the expansion of the Weddell Sea between South America and Antarctica, the formation of the small Scotia plate produced a strike-slip tectonic regime along the Fuegian Andes (Cunningham, 1993, 1995). Since then, this transform boundary accommodates the relative movement between the plates of South America and Antarctica (Cunningham, 1995). During the Cenozoic especially, a left-lateral wrench deformation affected the southern sector. The structures associated are mainly transtensional with extensional faults and the development of pull-apart basins along the main wrench faults (Lodolo *et al.,* 2003; Menichetti *et al.,* 2008). One of the main lineaments associated with this tectonic regime is the WNW-ESE 100 km long Valle Carbajal located in the central part of the Fuegian Andes (Cenni *et al.,* 2006) that split the Andean chain in two sectors, *i.e.,* the Sierra Alvear in the north and the Sierra Sorondo in the south (Fig. 2).

This contribution deals with the Mesozoic record of central Tierra del Fuego (Argentine) in the area bounded by the Lago Fagnano to the north and the Canal Beagle to the south, and from Paso Garibaldi in the east to the Bahía Ensenada in the west (Fig. 2). The main units exposed in this area belong to the Lemaire and Yahgán formations. The Lemaire Formation (Olivero *et al.,* 1999; Olivero and Martinioni, 2001) consists of acidic to mesosilic volcanic-pyroclastic rocks and basalts, and associated sedimentary rocks. This volcano-sedimentary complex has been interpreted as the record of the Late Jurassic extensional regime that led to the formation of the Rocas Verdes marginal basin (Katz, 1972; Dalziel *et al.,* 1974). It is characterized as a submarine complex that includes sedimentary rocks (conglomerates, chert, and black radiolarian and carbonaceous mudstones), acid volcanic and volcaniclastic rocks and basaltic facies representing the oceanic crust of the basin (Bruhn, 1979; Hanson and Wilson, 1991; Olivero and Martinioni, 2001). The main outcrops are found along a discontinuous WNW belt from Sierra Alvear to Isla de los Estados and in a restricted area at Bahía Ensenada. The monotonous 6,000 m thick, deep- marine black mudstones, including andesitic volcaniclastic turbidites and tuffs of the Lower Cretaceous Yahgán Formation were deposited in the Rocas Verdes Basin (Bruhn, 1979; Caminos *et al.,* 1981; Olivero *et al.,* 1999; Olivero and Martinioni, 2001). This unit is exposed along a WNW-ESE trending belt north of Canal Beagle (Fig. 2).

The Lower Cretaceous Beauvoir Formation (Fig. 2) completes the Mesozoic infilling of the RVB; it outcrops along a WNW-ESE trending belt extending from the eastern Lago Fagnano to the Atlantic coast. The Beauvoir Formation is chiefly made of dark slates and tuffs with minor sandstones, interpreted as derived from crustal basement on the continental side of the Rocas Verdes Marginal Basin (Olivero and Martinioni, 2001; Olivero *et al.,* 2009).

3. Structures

Two deformational events developed during the inversion of the Rocas Verdes Basin (Dalziel and Palmer, 1979; Bruhn, 1979). The first one occurred during the Late Cretaceous and produced (F_1) folds and slaty cleavage (S_1). During this deformation, the rocks were affected by prenhite-pumpellyte to greenschist facies metamorphism (Kohn *et al.,* 1993, 1995). The second deformational event is associated with the formation and emplacement of NE verging fold-and-thrust systems (Bruhn, 1979; Menichetti *et al.,* 2008) which originated large F_2 folds with a well-developed, non penetrative crenulation cleavage (S_2).

The compressive tectonics of the Fuegian Andes is characterized by north-verging imbricate structures, progressively translated along a sole thrust rooted in the Upper Jurassic to Cretaceous mudstone and slate levels (Figs. 3 and 4). The thrust surface is characterized by a brittle shear zone a few tens of meters thick where S/C tectonites are very well developed. In Sierra Alvear, the compressive structures merge in thick mylonitic shear zones formed in sub-greenschist metamorphic conditions. The geometry of the thrust complex is an upright, south dipping monocline of moderately tilted sedimentary strata (Fig. 4). The thrust surfaces are located in the marls levels of both the Upper Jurassic and the Cretaceous rocks. Two main coaxial populations of macro-and mesoscale structures trending WNW-ESE can be identified: **1.** large folds and low-angle to bedding-parallel thrusts/décollements and **2.** asymmetric chevron folds (Fig. 5a) and moderately steeply SSW dipping thrusts that form part of the major fold-and-thrusts belt system. Cumulative shortening of these structures could be estimated in tens of kilometers across the region (Menichetti *et al.,* 2008).

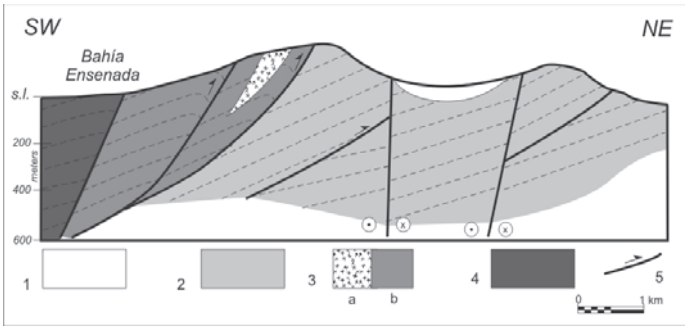

FIG. 3. Geological cross section of the Bahía Ensenada area. Location in figure 2. **1.** Quaternary (fluvio-glacial sediments); **2.** Yahgán Formation (Lower Cretaceous); **3.** Lemaire Formation (Upper Jurassic). **a.** basaltic facies; **b.** acid tuffs and ignimbrites; **4.** Lapataia Formation (pre-Jurassic?); **5.** Fault.

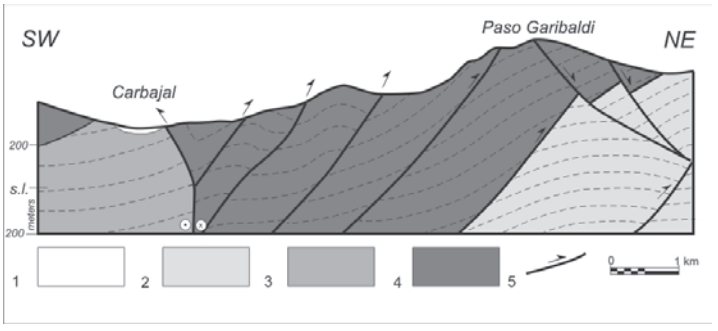

FIG. 4. Geological cross section from Valle Cabajal to Paso Garibaldi. Location in figure 2. **1.** Quaternary (fluvio-glacial sediments); **2.** Beauvoir Formation (Lower Cretaceous); **3.** Yahgán Formation (Lower Cretaceous); **4.** Lemaire Formation (Upper Jurassic); **5.** fault.

The main phase Andean folds and slaty cleavage and their relationship with the D_2 structures are well exposed in the SW of the studied area (Bahía Lapataia and Ensenada area) as well as north of Ushuaia in Valle Carbajal, up to Paso Garibaldi and Lago Fagnano area. The slaty cleavage affecting all formations has a NW-SE trend and dips towards the south. The fold axes trend from SSE-NNW for F_1 to ESE-WNW for F_2, both with axial planes generally dipping SW (40°-60°). In the Lemaire and Yaghán formations located in the Ushuaia area, the slaty cleavage locally features south to south-west dipping extensional lineations that are defined by the alignment and stretching of micaceous minerals and porphyroclasts. The crenulation cleavage S_2 is well developed in the basement rocks with a NE-SW trend dipping towards SE at a high angle.

In the Bahía Ensenada area (Fig. 3) in the northern shore of the Canal Beagle, the structures are dominated by several NE-verging thrusts, the southernmost of which places the basement rocks of Lapataia Formation over the Jurassic-Cretaceous units (Lemaire and Yahgán formations). Thrusts in turn are offset by W-E trending faults, likely pertaining to the sinistral strike-slip Canal Beagle Fault System (Fig. 2; Cunningham, 1993, 1995).

The Valle Carbajal represents one of the main E-W morphostructural lineaments in central Tierra del Fuego. The main structures are associated with the left-lateral strike-slip faults that produced a set of 'en echelon' positive structures along the valley (Cenni *et al.,* 2006). In the south-western side, a low angle fault rooted in black-shales overthrusts for few kilometers the Lemaire Formation over the Yaghán Formation (Fig. 4). In the center of the valley a left lateral strike-slip fault produces an oblique syncline where several mesoscopic folds with E-W sub-horizontal axes are strongly deformed by a subvertical axial plane pervasive cleavage (Menichetti *et al.,* 2004). Few imbricate duplexes of the Lemaire Formation affected the SW limb of Paso Garibaldi with thrust surfaces that display low angle S/C structures (Fig. 5b).

In the area of Paso Garibaldi, the main compressive structures associated with the Andean orogenesis are overprinted by the extensional faults related to the strike-slip system of the Magallanes-Fagnano fault (Menichetti *et al.,* 2004). Here, the lithological assemblage of the Lemaire Formation is represented by strongly foliated black shales enveloping several sigmoidal structures of tectonically deformed basaltic rocks. Shear structures mark the boundary of the

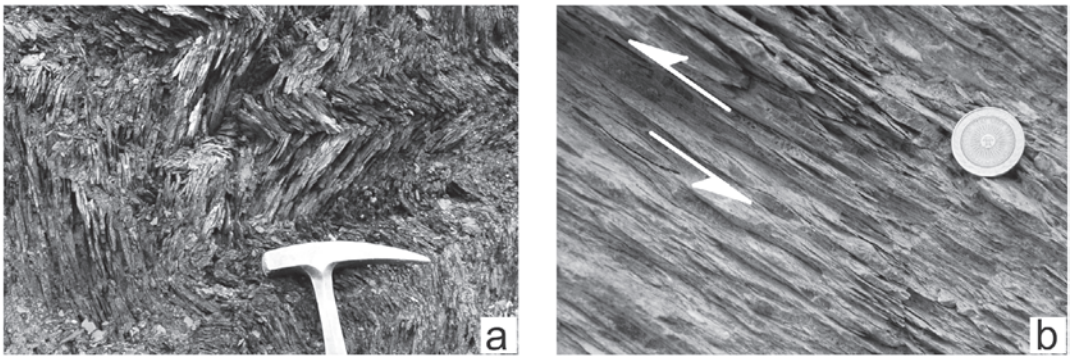

FIG. 5. **a.** Folds with sub-horizontal axial plane associated with the thrust shear zone in the SW limb of the Sierra Alvear; **b.** S and C structures in the compressive shear zone in the Lemaire Formation in the Paso Garibaldi area.

basaltic lenses and the fine-grained metaclastic/ metavolcaniclastic host, both showing refraction of the cleavage planes. The system of thrust faults is cut by NE-dipping normal faults with an offset of a few hundred meters (Menichetti *et al.,* 2004; Fig. 4).

4. Petrography/microstructures

4.1. Lemaire Formation

Rock exposures of the Lemaire Formation in Sierra Alvear show dismembered fragments of the oceanic crust and deep infilling of the RVB. The basic volcanic rocks of central Tierra del Fuego have been interpreted as dikes and sills flanking the outcrop belt of ophiolites in the southern archipelago (Tortuga Complex) and would represent an early phase of the igneous-tectonic event which led to the formation of the mafic portion of the floor of the back-arc basin (Bruhn *et al.,* 1978; Stern, 1980). Within the studied area the rocks of the Lemaire Formation are characterized by strong deformation within the ductile regime and lower greenschist facies assemblages.

The lowermost levels of the Lemaire Formation are represented by highly deformed siliceous tuffs and ignimbrites. These rocks are characterized by the presence of highly elongated fiamme-like lenses along with primary quartz and feldspar crystaloclasts and replaced pumiceous fragments somewhat tectonically rounded. The penetrative mylonite foliation is usually defined by high aspect ratio white mica, often accompanied by minor chlorite, carbonate and discontinuous seams of insoluble material. A suite of brittle microstructures is shown by feldspar porphyroclasts (book-shelf, microboudinage) (Fig. 6A). Quartz strain fringes associated with tiny pyrite cubes as well as microboudinage in feldspar porphyroclasts are widespread in the Valle Carbajal outcrops and indicate a roughly W-E extensional component.

The metavolcaniclastic rocks are overlain either by marine metasediments or by basic rocks representing the oceanic crust of the RVB (Cerredo *et al.,* 2007). Marine sedimentation is represented by black shales with sparse siliceous oozes and occasional interlayers of bedded chert horizons which indicate sedimentation in deep ocean areas. The very fine-grained shales display metamorphic layering and often preserve relics of a S_0 earlier anisotropy within microlithons of penetrative S_1 foliation defined by insoluble dust opaque material. Pre-S_1 extensional quartz-pyrite veins have been folded; pyrite is also abundant within the rock matrix and typically associated with strain fringes (either of quartz or quartz-chlorite-muscovite assemblages).

Thin, discontinuous levels of black shales are also found interlayered within basic tuffs and lavas. The basic tuffs typically display a profuse vein network dominated by sea-floor metamorphism mineral assemblages (calcite-quartz-opaque minerals). The tuffs are composed of lithic volcanic fragments of either porphyric texture or glassy with embryonic crystals, pumiceous fragments, glass shards and rare broken plagioclase crystaloclasts. Some tuffaceous layers contain significant proportions of non-volcanic biogenic particles (*i.e.,* siliceous oozes and spheroidal polycrystalline sphene). Intense deformation resulted in mylonitic microstructures where former lithic fragments and plagioclase clasts have been transformed in porphyroclasts, often displaying microboudinage (Fig. 6B) and book-shelf textures; pumiceous fragments in turn, have been smeared out by deformation. In the most strained domains

oriented high-aspect ratio chlorite define the mylonite foliation and wrap around calcite porphyroclasts with core and mantle structure.

Two groups of coherent basaltic to basaltic-andesitic rocks are distinguished within the oceanic igneous component of RVB crust: a plagioclase-phyric (to aphyric) vesicle-rich facies, and an ophitic facies (either porphyric or aphyric) vesicle-poor facies. Primary texture and mineralogy of different lithologies have been severely modified by a former sea-floor metamorphism, later overprinted by oriented greenschist facies associations related with the Andean tectonics (Cerredo *et al.,* 2008). The poorly vesicular ophitic rocks show scarce vugs and generally preserve chlorite-zoisite±zeolite assemblages related to sea-floor metamorphism, rarely amphibole occurs as coronas around clinopyroxene. Magmatic phenocrysts have been transformed into porphyroclasts variably rotated into parallelism with the tectonic foliation defined by chlorite+fibrous prehnite±muscovite assemblages (Fig. 6C).

Plagioclase-phyric basalts are generally vesicle-rich; sea-floor metamorphism is mostly restricted to unoriented vesicle filling assemblages (chlorite, chlorite-zoisite, chlorite-zoisite-carbonate-opaque mineral, zoisite-laumontite-opaque mineral-prehnite). The microstructural overprint resulting from Andean tectonics is chiefly located within these soft mineral associations which have been variably reoriented and/or recrystallized (Fig. 6D).

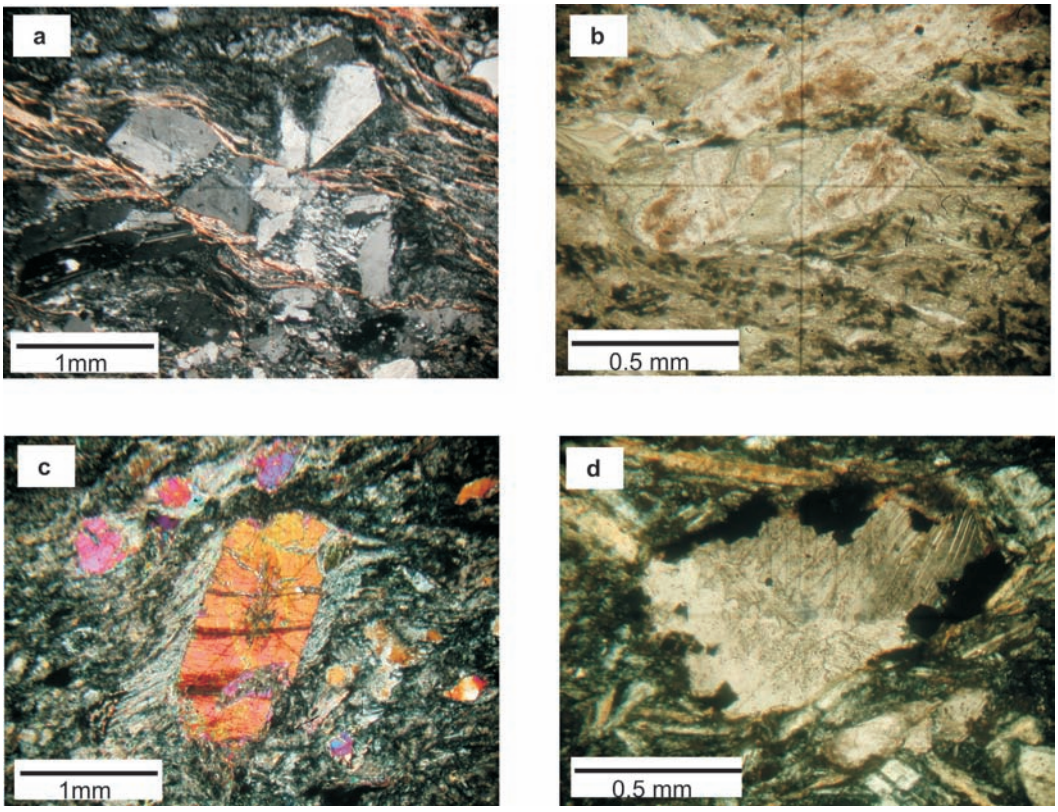

FIG. 6. Photomicrographs of typical microstructures in the different lithologies of the Lemaire Formation; sections were cut normal to the magnetic foliation and parallel to the magnetic lineation. All photographs were taken under crossed polars. **a**. Siliceous tuff of Sierra Alvear with microboudinadged plagioclase; fine-grained syntectonic quartz occupies boudin-necks. Foliation is delineated by high-aspect ratio white mica; **b.** Basic tuff of Paso Garibaldi. Intense deformation has transformed former plagioclase crystalloclast in microboudinadged porphyroclast. Oriented chlorite-prehnite association is found filling boudin-neck, in pressure shadow areas and delineating the foliation; **c.** Ophitic basalt from western Valle Carbajal displaying typical microstructure with clinopyroxene porphyroclasts partially enveloped by prehnite pressure-shadows; **d.** Carbonate-opaque mineral assemblage filling a vesicle in plagioclase-phyric basalt (near Paso Garibaldi). Although rock is dominated by a primary magmatic microstructure, calcite twining and subgrain development attest deformation.

4.2. Yahgán Formation

The single AMS site belonging to the Yahgán Formation comes from Monte Olivia area (Fig. 2) and corresponds to thin layers of black mudstones within basaltic rocks. The subvolcanic igneous rocks of Monte Olivia intruded in the Yahgán Formation just below the tectonic contact with the Lemaire Formation (Olivero and Malumián, 2008; Olivero *in* Menichetti *et al.,* 2004). The mudstones are dominated by silty particles with rare medium- to fine-grained volcanic feldspar and quartz clasts often accompanied by siliceous oozes. Elongated recrystallized quartz in thin veins along with oriented opaque minerals characterizes the foliation.

5. Anisotropy of magnetic susceptibility (AMS)

A systematic sampling of the different lithologies of the Lemaire Formation was carried out. It comprised 27 sites (two hundred and forty samples), including one site at the Yahgán Formation (Fig. 2). Several oriented samples of 2.54 cm in diameter and 5 to 9 cm long, were collected at each site with a portable drill. Samples were oriented with both sun and magnetic compasses whenever possible. At each site, a detailed structural survey of foliation planes, fractures and veins was done in order to help in the interpretation of the AMS data. The collected cylinders were sliced in the laboratory in order to obtain 2.2 cm long standard specimens. Measurements of the susceptibility tensor were done with the MFK1-B Kappabridge at the INGEODAV ('Departamento de Ciencias Geológicas, Universidad de Buenos Aires'). Each sample was measured at fifteen different positions, and then the susceptibility tensor was fit to the results. The AMS ellipsoid for each site was computed according to Jelinek (1977, 1978). Geometric means of bulk susceptibility (κ) were computed for each site. Mean site data are presented in Table 1 and Figs. 7 and 10.

5.1. Bulk susceptibility (κ)

The acidic tuffs and ignimbrites of the Lemaire Formation present κ values falling in the paramagnetic field (Tarling and Hrouda, 1993). Values range between 6 and 64 x 10^{-5} SI units. Given that the mineralogy of this rock type is dominated by diamagnetic minerals (*i.e.,* quartz and feldspars) and

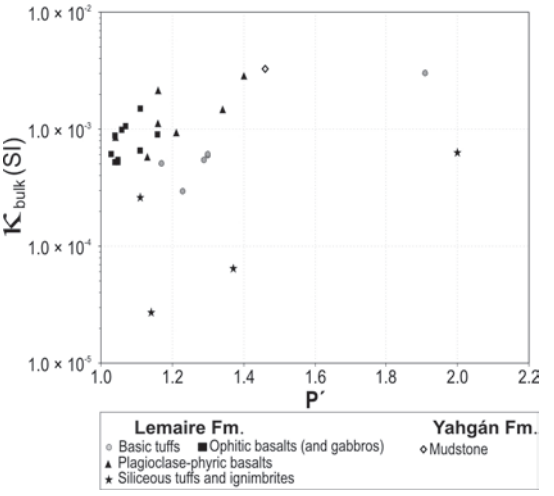

FIG. 7. κ_{bulk} (site average mean bulk susceptibility) *versus* P´ (anisotropy degree) plot for each site with indication of lithology.

the low content of paramagnetic components (<5%), it is probable that the susceptibility parameters are governed by a minute fraction of a ferromagnetic mineral.

The three groups of basic rocks share similar bulk susceptibility ranges but display distinct trends in the κ *versus* P´ plot (Fig. 7). All groups display susceptibility values in the range considered to be governed both by paramagnetic and ferromagnetic components (Tarling and Hrouda, 1993), but, whereas the ophitic rocks show fairly well clustered values between 23 and 114x10^{-5} SI units over a restricted P´ range (1.03-1.16), the plagioclase-phyric rocks display a trend toward higher κ values (58 to 283x10^{-5} SI units) within a wider range of anisotropy degree (1.04-1.4). The basic tuffs, in turn, present a similar susceptibility range (50-298x10^{-5} SI units) associated with the largest span in P´ (1.16-1.9). The large scatter in bulk susceptibility values of the plagioclase-phyric lavas and basic tuffs could be correlated with a wide petrographic variation linked to post-emplacement processes (vesicle and fracture filling assemblages).

5.2. Magnetic Properties

Five samples, representing different lithologic types, were chosen for rock-magnetic tests in order to identify the ferromagnetic minerals (Figs. 8 and 9). Selected samples were: F4.3, F7.8, F9.4, F11.4

(of the Lemaire Formation) and Y7.3 (of the Yahgán Formation). The tests consisted in measuring the variation of magnetic susceptibility (κ) with temperature (between -194ºC and ≈700ºC) and with the applied magnetic field (H, between 2 and 700 A/m). Both sets of measurements were done with the MFK1-A Kappabridge and its implements of low and high temperature at the INGEODAV. For both procedures, the samples were reduced to fine-sand size with a hammer and a mortar agate.

TABLE 1. MEAN SITE AMS DIRECTIONAL AND SCALAR VALUES FOR THE FUEGIAN ANDES.

Site	N	κ_{mean} (10^{-5} SI)	κ1		κ2		κ3		P´	T	Lithology
			Dec (º)	Inc (º)	Dec (º)	Inc (º)	Dec (º)	Inc (º)			
F7	13	63.8	245	71	147	3	56	19	2.00	0.40	(LF)-Siliceous tuffs and ignimbrites
F12 B	7	2.7	303	47	87	37	192	19	1.14	0.39	(LF)-Siliceous tuffs and ignimbrites
Y6	7	6.5	242	64	117	16	21	21	1.37	0.23	(LF)-Siliceous tuffs and ignimbrites
GME5	5	26.2	142	25	271	53	40	25	1.11	0.18	(LF)-Siliceous tuffs and ignimbrites
F5	12	54.4	237	28	144	4	47	61	1.05	0.13	(LF)-Ophitic basalts (gabbros)
F8	12	60.6	215	34	112	19	358	50	1.03	-0.16	(LF)-Ophitic basalts (gabbros)
F9 A	4	Not enough records for meaningful statistics (Jelinek, 1978)									(LF)-Ophitic basalts (gabbros)
F12 A	5	51.6	127	7	240	73	35	16	1.05	0.01	(LF)-Ophitic basalts (gabbros)
F13	10	52.2	291	54	100	36	194	5	1.04	-0.15	(LF)-Ophitic basalts (gabbros)
Y2	6	88.5	192	19	288	17	58	64	1.16	-0.02	(LF)-Ophitic basalts (gabbros)
Y3	5	88.2	169	38	46	35	290	33	1.04	-0.83	(LF)-Ophitic basalts (gabbros)
Y4	8	97.2	219	44	316	7	52	45	1.06	0.71	(LF)-Ophitic basalts (gabbros)
Y9	5	105.0	116	5	217	66	24	23	1.07	0.35	(LF)-Ophitic basalts (gabbros)
Y10	8	64.6	141	32	239	12	347	55	1.11	0.39	(LF)-Ophitic basalts (gabbros)
GME3	6	150.0	244	52	22	30	125	21	1.11	-0.04	(LF)-Ophitic basalts (gabbros)
F6	10	92.5	199	57	309	12	46	31	1.21	0.01	(LF)-Plagioclase-phyric (or aphyric) basalts
GME1	14	83.3	191	33	301	28	57	44	1.04	0.15	(LF)-Plagioclase-phyric (or aphyric) basalts
Y1	5	312.0	254	18	157	22	21	61	1.40	0.56	(LF)-Plagioclase-phyric (or aphyric) basalts
Y5	6	145.9	261	18	150	48	5	37	1.34	-0.03	(LF)-Plagioclase-phyric (or aphyric) basalts
Y8	9	58.5	116	13	324	76	207	7	1.13	0.36	(LF)-Plagioclase-phyric (or aphyric) basalts
F3	10	112.2	181	48	299	23	45	33	1.16	-0.25	(LF)-Plagioclase-phyric (or aphyric) basalts
GME4	7	214.0	195	34	318	39	79	33	1.16	0.55	(LF)-Plagioclase-phyric (or aphyric) basalts
F1	6	54.2	198	9	291	19	85	69	1.29	0.63	(LF)-Basic tuffs
F2	6	59.0	196	8	290	23	87	66	1.30	0.60	(LF)-Basic tuffs
F4	21	298.5	185	38	300	29	56	39	1.91	0.03	(LF)-Basic tuffs
F9 B	7	28.9	215	39	108	20	357	44	1.23	0.15	(LF)-Basic tuffs
F10	9	50.5	243	37	127	31	9	38	1.17	0.62	(LF)-Basic tuffs
F11	11	59.9	62	5	169	75	331	15	1.30	0.30	(LF)-Basic tuffs
Y7	6	329.4	291	14	144	73	23	9	1.46	0.21	Fm Yahgán: Pelite

N: Number of independent cores per site used to compute mean; κ: A geometric mean of the magnetic susceptibility; **T:** Shape anisotropy factor, **P´:** Corrected anisotropy degree as defined by Jelínek (1981); **Lf:** Lemaire Formation.

Two different behaviors can be recognized in figure 8. One set of samples (F9.4 and F11.4) show no significant variations of the bulk susceptibility with the applied field. Instead, the other samples (F4.3, F7.8 and Y7.3), show an increase in susceptibility with applied field. This behavior is indicative of coarse-grained (typically hundreds of micrometers) pyrrhotite, hematite or titanomagnetite (Hrouda, 2002). In figure 9A, the thermomagnetic curves of samples F4.3, F7.8 and Y7.3 show a clear Hopkinson peak at ≈320ºC. Petrovký and Kapička (2006) suggest that the temperature of a sharp Hopkinson peak can be used as the Curie point. Therefore we infer the presence of pyrrhotite (mixture of monoclinic and hexagonal; Dunlop and Özdemir, 1997; Martín-Hernández *et al.,* 2008). The rise of κ around 500ºC probably corresponds to the breakdown of pyrrhotite into magnetite (Dunlop and Özdemir, 1997; Martín-Hernández *et al.,* 2008). Consequently, it is inferred that the magnetic behavior of these samples (F4.3, F7.8 and Y7.3) is governed by pyrrhotite. On the other hand, samples F9.4 and F11.4 exhibit a clear hyperbolic decay with temperature (Fig. 9B) which indicates the dominance of paramagnetic minerals. A minor rise on κ at ≈315ºC suggests a relatively small presence of pyrrhotite. Irrespective of the characterization of the samples as dominated by ferrimagnetic (pyrrothite) or paramagnetic minerals, no significant differences in the AMS parameters was observed, with the possible exception of P´, much higher in the pyrrothite dominated samples (see below)

5.3. AMS scalar parameters

The anisotropy degree (P´) and shape parameter (T) were computed following Jelínek (1978) and are shown in figure 10. When the whole collection is considered no significant correlation between P´ and bulk susceptibility is observed (Fig. 7).

P´ values in the acid tuffs and ignimbrites of the Lamaire Formation are highly variable, spanning from 1.09 up to 2. For this lithology the AMS ellipsoid is oblate (T>0) and no correlation can be established between anisotropy degree and shape parameters. Within the basic rocks, the ophitic basalts display the most clustered and consistently low P´ values. The lowest anisotropy degrees (<1.04) are associated with prolate ellipsoids while higher P´ values relate with oblate ellipsoids. The plagioclase-phyric (or aphyric) basalts (and basaltic andesites) are

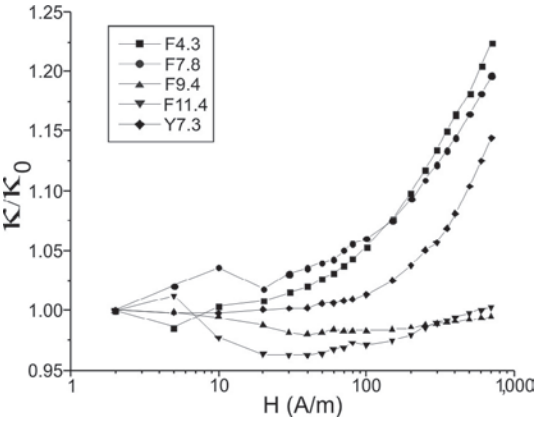

FIG. 8. Variation of susceptibility (κ/κ_0) with the applied magnetic field (H) for a selected group of the studied samples. To avoid problems with orders, the susceptibility normalized by the value of the susceptibility measured at 2 H is plotted against the field intensity. Two groups are distinguished: the one represented by samples F11.4 and F.9.4 show no significant variation with the applied field; instead samples F4, F7.8 and Y7.3 show a marked increase in magnetic susceptibility with the applied field.

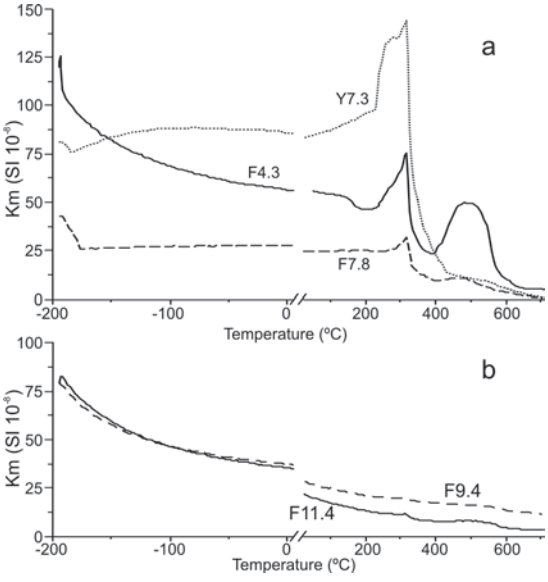

FIG. 9. Thermomagnetic curves (magnetic susceptibility *versus* temperature) between -194ºC and ≈700ºC. **a.** Samples F4.3, F7.8 and Y7.3 show a clear Hopkinson peak at ≈320ºC (indicating the presence of pyrrhotite) and a marked κ rise at around 500ºC; **b.** Samples F9.4 and F11.4 display hyperbolic susceptibility decay with temperature which indicates the dominance of paramagnetic minerals. A minor rise on κ at ≈315ºC suggests the presence of pyrrhotite in very minor amounts.

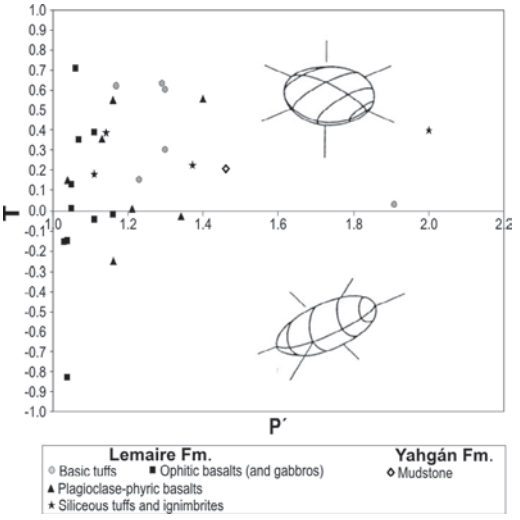

FIG. 10. T *versus* P′ diagram (Jelinek, 1981) for the studied sites. Note the predominance of oblate shapes. Symbols as in figure 4.

dominated by oblate ellipsoids, and show a strong correlation between P′ and κ which makes dubious any interpretation of P′ as indicator of deformation intensity. The basic tuffs present oblate ellipsoids and are characterized by a large span in the anisotropy degree (1.2-1.9).

The large range in P′ associated with a consistent AMS directional pattern (see below) is probably due to the varied lithology of the sampled rocks, although a heterogeneous strain can also be part of the explanation. The presence of numerous sites with anisotropy degrees exceeding 20% attest in favour of a magnetic fabric of tectonic origin (or at least affected by tectonic strain). The two anomalously high P′ values in sites F4 and F7 (Table 1) are due to the abundance of pyrrhotite (ferromagnetic mineral with high intrinsic anisotropy) as indicated by the thermomagnetic curves and relations of κ *versus* H (see Figs. 8 and 9). The performed thermomagnetic tests indicate that for samples with P′ values higher than 1.5 the magnetic properties are strongly governed by pyrrhotite. Instead samples yielding anisotropy degrees lower than 1.4, although with minor amounts of pyrrhotite (Fig. 9b) show a magnetic behaviour controlled by paramagnetic minerals (Figs. 8 and 9). As observed in thin sections, pyrrhotite is mostly located in veins (quartz-calcite) generally with deformation imprint (Fig. 6d). The control of the anisotropy degree by the amount of pyrrothite rules out a simple relation between P′ and degree of tectonic deformation in these sites.

5.4. AMS directional data

Distribution of κ_1, κ_2 and κ_3 are presented for each site in the stereonets of figure 11 along with the average plane and pole of mesoscopic foliation measured in the field at each site. Since many sites were located on thick volcanic bodies with no clear foliation planes, the slaty cleavage was measured in most cases in the host or intercalated metasediments in the volcano-sedimentary association of the Lemaire Formation. In general, the magnetic fabric directional data show a significant coherence and consistency within and between sites irrespective of the involved lithology. Furthermore, the different influence of ferrimagnetic (pyrrhotite) minerals in the AMS, as shown by the bulk κ values (Table 1; Fig. 7), does not have any significant effect in the directional data.

According to the pattern of AMS directional data and its relation with the tectonic fabric, the stereonets of figure 11 were grouped into three domains:

5.4.1. Domain I

Comprises the sites of the Lemaire Formation located along the N-S transect from Paso Garibaldi to Valle Carbajal where both field and AMS fabric are dominated by NW-SE striking foliations (slaty cleavage) with low to moderate dips towards the southwest. κ_3 is roughly coincident with the pole of the slaty cleavage, as measured in the field. The magnetic lineation (κ_1), although somewhat scattered, is generally subhorizontal to shallowly inclined and plunges roughly southwards (S, SSE or SSW). κ_1 axes show either a girdle distribution, characteristic of AMS oblate ellipsoids (*e.g.,* F1, F2, Y1, Y2, Y4) or are clustered within the plane of foliation producing triaxial AMS ellipsoids (*e.g.,* F3, F4, F5, GME1, Y3, F6, F7). At site F8 magnetic foliation is significantly shallower than the slaty cleavage foliation measured at the outcrop in the metasedimentary host, suggesting a possible refraction of the cleavage plane in the volcanic body.

5.4.2. Domain II

Includes the sites of the Lemaire and Yahgán formations located along the Valle Carbajal which show a distinct AMS pattern characterized by triaxial

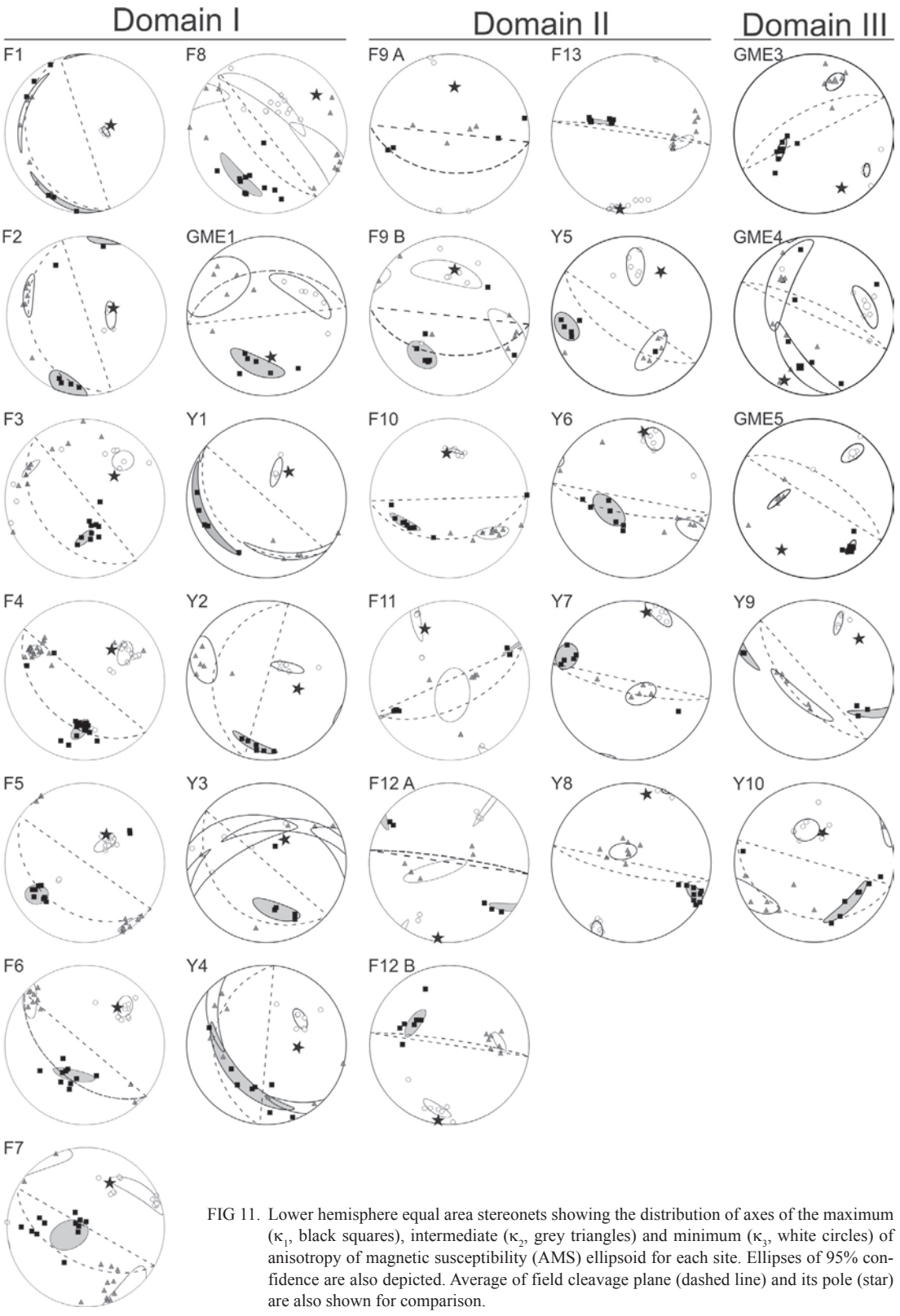

FIG 11. Lower hemisphere equal area stereonets showing the distribution of axes of the maximum (κ_1, black squares), intermediate (κ_2, grey triangles) and minimum (κ_3, white circles) of anisotropy of magnetic susceptibility (AMS) ellipsoid for each site. Ellipses of 95% confidence are also depicted. Average of field cleavage plane (dashed line) and its pole (star) are also shown for comparison.

ellipsoids and roughly E-W (WNW-ESE) steeply inclined (50° to 80°) magnetic foliation, dipping both southwards and northwards. The majority of magnetic lineations within this area are typically subhorizontal or shallowly dipping either towards the E-ESE or W-WNW. Although in some sites κ_1 axes cluster within the foliation plane in the down dip direction (F9B, F12B, F13, Y6), the distribution of κ_1 towards the strike direction within the foliation plane (F11, F12, Y7, Y8) is characteristic of this domain.

5.4.3. Domain III

The sites of the Lemaire Formation located in the Canal Beagle area show either triaxial or oblate AMS ellipsoids and display magnetic fabrics dominated by NW-SE to WNW-ESE/ ENE-WSW striking foliations with shallow and subordinated steep S/ SW inclinations; the large shift between magnetic foliation and average field foliation in some sites (GME4, GME5) points to the existence of a cryptic anisotropy not observed at outcrops. WNW-ESE oriented magnetic lineations with shallow (to moderate) plunges are either clustered along the strike of foliation (GME3, Y9) or form girdles within the foliation plane (Y10).

6. Discussion

The penetrative regional foliation of the Lemaire and Yahgán formations in the studied area of the Fuegian Cordillera is defined by very low grade metamorphic associations. From microstructural observations it was recognized that this foliation is associated with characteristic mineral assemblages for each lithological type. It is dominated by white mica in the acid tuffs and ignimbrites whereas chlorite (±prehnite±muscovite±opaque minerals) characterizes the penetrative cleavage in the basic terms –tuffs, lavas– of the Lemaire Formation. Field observations and analysis of oriented thin sections allowed establishing that magnetic fabrics clearly match with both the observed foliation and extensional lineations.

In Domain I the magnetic fabrics in the Lemaire Formation is generally dominated by foliations of NW-SE strike (Fig. 11) regardless of the involved lithology and the amount of pyrrhotite present. Magnetic foliations with low to moderate dips towards the southwest are roughly coincident with the penetrative foliation measured at each sampling site (Fig. 11). Furthermore, when all data of magnetic foliations are plotted in a single stereonet and compared with the foliations measured at outcrops for the same area, a striking correspondence emerges (Fig. 12).

In spite of some dispersion, the magnetic lineation shows mostly subhorizontal to shallow plunges towards the S, SSE or SSW, which is consistent with the mineral lineation assigned to the main phase of Andean deformation (D_1, Bruhn, 1979; L_1, Menichetti *et al.,* 2008). The common clustering of magnetic lineations on the surface of foliation in the down-dip direction can be interpreted as a transport or stretching fabric (Fig. 11). Further support for this interpretation is provided by the recognized extensional microstructures parallel to κ_1 (microboudinage, book-shelf, etc. Fig. 6).

Despite excellent agreement showed by magnetic and field foliations (Fig.12), comparison of stereonets representing all magnetic lineations within this domain and the correspondent data measured on outcrop (*i.e.,* striae on fault surfaces) does not yield fully coincident patterns (Fig. 12). The main clustering of subvertical striae is related to thrust faults and the secondary clusters of subhorizontal striae are associated with the strike-slip structures. Fuegian thrust propagation took place in several pulses from Late Cretaceous to Miocene times (Ghiglione and Ramos, 2005 and references therein) and it is generally accepted that strike slip faulting within this area had a major role since Oligocene onwards (Klepeis and Austin, 1997). Given that magnetic fabric is linked to the earliest orogenic stage (and associated penetrative deformation and metamorphism) in the Late Cretaceous, we interpret that striae measured at outcrop as belonging to Tertiary tectonics in the axial zone of the Fuegian orogen.

The roughly E-W segment of the AMS transect along Valle Carbajal (Domain II) shows the predominance of E-W striking magnetic foliations (steeply dipping either N or S) over the NW-SE trending ones (Fig. 11). Field foliation in the Lemaire and Yahgán formations nearly mimics the magnetic foliation within this domain (Fig. 12). Magnetic lineations are represented by clustering of κ_1 axes mostly along foliation strike (Fig. 11) dominantly subhorizontal to shallowly plunging (either eastwards or westwards). Their overall distribution closely matches with that of striae of strike slip faults (Fig. 12).

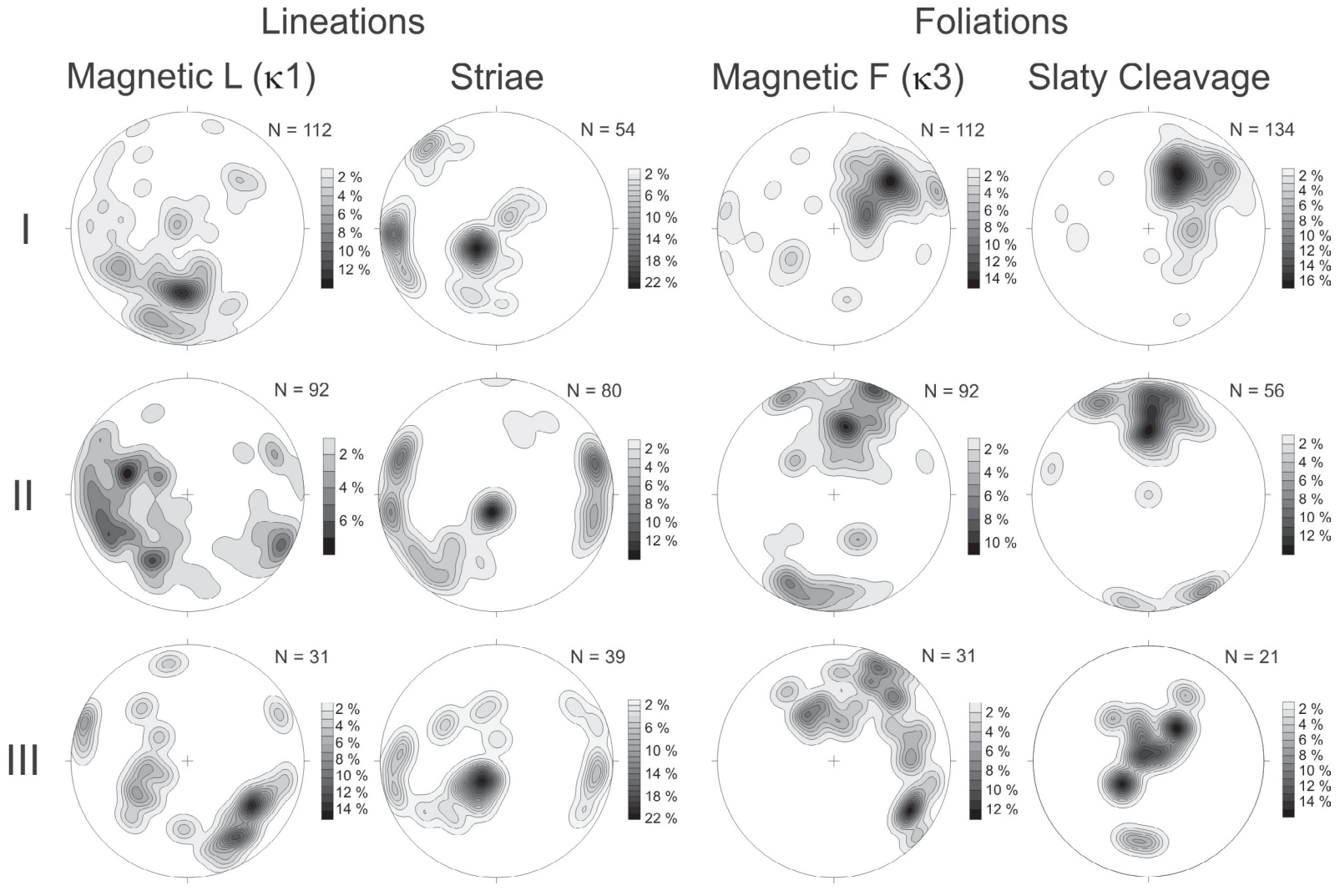

FIG 12. Lower hemisphere equal area stereonets representing the total data of magnetic foliations and lineations for each of the defined domains, data of field foliations and lineations (mainly striae on fault surfaces) for the same domains are also shown for comparison.

Only a few E-W mineral lineations have been previously reported for the Lemaire Formation exposed in the area of Valle Carbajal (Bruhn, 1979), but the dominance of subhorizontal magnetic lineations within subvertical foliation planes that appears as a representative character of the magnetic fabric in this area, along with the statistical coincidence between the maxima of magnetic lineation and striae on strike-slip faults suggests that the magnetic fabric may be associated with deformational processes of a transcurrent tectonic regime along the Valle Carbajal. Given that the magnetic fabric is associated with regional metamorphism which in turn is linked to the Late Cretaceous Andean deformation, the AMS pattern found in this domain may suggest that strike slip deformation along this valley is not only restricted to Late Cenozoic times.

The few AMS sampling sites of the Lemaire Formation located in the Bahía Ensenada area (Domain III) do not show such distinct pattern as the two domains described before, and any conclusion is therefore tentative. The field foliation data show a dominant NW oriented moderately dipping foliation (either to the NE or the SW). Instead, the distribution of magnetic foliations displays prevailing NW-striking planes with fairly constant SW dip of moderate to high angle (Fig. 12).

Magnetic lineations generally form clusters along strike (Fig. 11) with characteristic shallow plunge (E-NE, E-SE and W-NW); this κ_1 distribution might be related to roughly E-W strike-slip tectonics given the correspondence between magnetic lineation maxima and striae measured on transcurrent faults (Fig. 12). Less frequent moderately to steeply dipping magnetic lineations may relate to high angle inverse faults (Fig. 3). Different generation of fractures and quartz veins are present in the area (Menichetti *et al.,* 2008), often associated with the Canal Beagle left lateral strike-slip fault system (Cunningham, 1995) as well as the Late Cretaceous intrusions (Peroni *et al.,* 2009).

Strike-slip deformation has been generally assigned to Late Cenozoic transcurrent faulting in Tierra del Fuego (*e.g.,* Klepeis and Austin, 1997; Lodolo *et al.,* 2001 and references therein). However, it has been long recognized the transpressional nature of the closure and inversion of the Rocas Verdes Basin during the Late Cretaceous (Cunningham *et al.,* 1995; Klepeis and Austin, 1997; Peroni *et al.,* 2009). A component of left-lateral wrenching was identified for the Cretaceous of the Fuegian Cordillera and foot-hills (Nelson *et al.,* 1980; Cunningham, 1995; Diraison *et al.,* 1997), related to the relative motion between South America and the Antarctic Peninsula (Cunningham *et al.,* 1995; Klepeis and Austin, 1997). Our results suggest that this possibility should be further investigated, since it might have had a role of some importance in the development of the Fuegian orogen. In this connection, we suggest that the role of Early Jurassic extensional structures during Andean compression should be also taken into account given that they represent zones of weakness which, under suitable orientation, may be reactivated as strike-slip faults within an overall compressive stress field. Both field data (Letouzey, 1990) and analog experiments (Del Ventisette *et al.,* 2006) show that reactivation of normal faults in an oblique compressional setting generates several types of deformation partitioning. Low angles (*i.e.,* <45º) between the preexisting normal fault systems and the shortening direction may result in thrusts in association with strike-slip faults (Brun and Nalpas, 1996).

A simplified conceptual model (Fig. 13) during the Late Cretaceous is proposed for the investigated area. The three domains interpreted from magnetic and structural grounds are represented as distinct segments characterized by the dominance of either contractive or transcurrent motions. The major factors responsible for this deformation partitioning deserve further research.

7. Conclusions

An AMS survey across the Fuegian Andes, based on over 240 samples from 27 sites has indicated that the magnetic fabric reflects the tectonic deformation that has affected the Mesozoic rocks in the region. Sampled rocks were mostly from the Late Jurassic Lemaire Formation and comprised volcanic, and pyroclastics rocks, with a single site in clastic sedimentary rocks of the Early Cretaceous Yahgán Formation. All rocks show low-grade metamorphism paragenesis associated with tectonic deformation. The analysis of oriented thin section analysis provided the necessary petrographic control to interpret the magnetic fabric data.

A large span in anisotropy degree from 1.04 up to 2.0 was observed. Although a heterogeneously distributed strain may have influenced P′ values, no significant correlation was observed between these

and the degree of deformation. Most measurements are consistent with a fabric of tectonic origin, as also interpreted from microstructural analysis and observed correlation between magnetic and tectonic foliation planes.

At most sites the magnetic foliation was consistent with the tectonic-metamorphic foliation (basically the slaty cleavage) providing extra confidence in the geologic interpretation of the AMS information. Despite a large lithologic variety, AMS directional data is rather consistent and can be interpreted as reflecting the dominant tectonic regime that affected the rocks in different sectors of the orogen. According to that, three domains have been defined (Figs. 11, 13). The first, encompassing the area from Paso Garibaldi to the Valle Carbajal, shows a magnetic fabric interpreted to have been formed by NE-SW Andean contractional deformation and development of the NE verging fold and thrust belt during the Late Cretaceous, with κ_1 associated with mineral lineations. A second domain (located along the Valle Carbajal) showed a magnetic fabric consistent with deformation governed by strike-slip tectonics. The third domain, close to the Canal Beagle shows a more complex pattern, but with evidence of E-W strike-slip deformation in the magnetic fabric.

Since it is generally accepted that the strike-slip regime along the Valle Carbajal and the Canal Beagle was active only in post-Paleocene times, further investigations on the possible existence of localized E-W strike-slip tectonics during the Late Cretaceous main Andean collisional orogeny as suggested herein should be investigated.

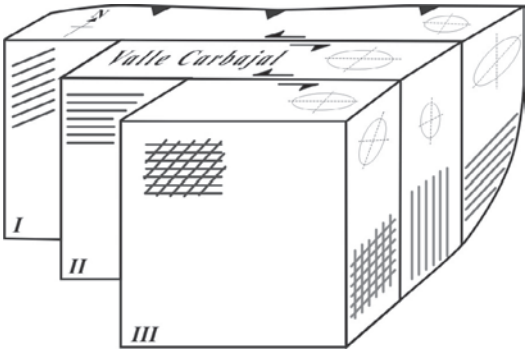

FIG 13. Schematic block diagram of the three domains (I, II, III) with indication of average magnetic lineations (black lines), foliations (grey lines) and the magnetic ellipsoids.

Acknowledgements

This study was supported by grants from Agencia Nacional Científica y Tecnológica, FONCyT. 2007, PICT 00106 (IDAC-ICES) and PICT 00434. The authors thank Estación Astronómica Río Grande (EARG) for the logistical and technical support in the field. We also acknowledge C.A. Vásquez and J.I. Peroni for their constant help in the laboratory work. We are grateful for the thorough and constructive reviews of the two anonymous referees which greatly improved the original manuscript.

References

Borradaile, G.J.; Henry, B. 1997. Tectonic applications of magnetic susceptibility and its anisotropy. Earth-Science Reviews 42 (1-2): 49-93.

Bruhn, R.L. 1979. Rock structures formed during back-arc basin deformation in the Andes of Tierra del Fuego. Bulletin of the Geological Society of America 90: 998-1012.

Bruhn, R.L.; Stern, C.R.; de Wit, M. 1978. Field and geochemical data bearing on the development of a Mesozoic volcano-tectonic rift zone and back-arc basin in southernmost South America. Earth and Planetary Science Letters 41: 32-45.

Brun, J.P.; Nalpas, T. 1996. Graben inversion in nature and experiments. Tectonics 15: 677-687.

Calderón, M.; Fildani, A.; Hervé, F.; Fanning, C.M.; Weislogel, A.; Cordani, U. 2007. Late Jurassic bimodal magmatism in the northern sea-floor remnant of the Rocas Verdes basin, southern Patagonian Andes. Journal of the Geological Society 164 (5): 1011-1022. DOI: 10.1144/0016-76492006-102.

Caminos, R.; Haller, M.; Lapido, O.; Lizuain, A.; Page, R.; Ramos, V. 1981. Reconocimiento geológico de los Andes Fueguinos. Territorio Nacional de Tierra del Fuego. *In* Congreso Geológico Argentino, No. 8, Actas 3: 759-786. San Luis.

Cenni, M.; Menichetti, M.; Mattioli, M.; Lodolo, E.; Tassone, A. 2006. Analisi meso-microstrutturale lungo la faglia trascorrente Magellano-Fagnano nella Cordigliera delle Ande in Terra del Fuoco-Argentina. Rendiconti della Società Geologica Italiana. Nuova Serie 2: 121-124.

Cerredo, M.E.; Remesal, M.B.; Tassone, A.; Menichetti, M. 2007. The ocean crust of Rocas Verdes Basin in Tierra del Fuego, Argentina. *In* Simposio Argentino del Jurásico, No. 3, Actas 1: 33. Mendoza.

Cerredo, M.E.; Menichetti, M.; Remesal, M.B.; Tassone, A. 2008. Rheological control on the development of

shear zones: a case study of the ophiolitic assemblages in central Tierra del Fuego, Argentina. *In* Congreso Geológico Argentino, No. 17, Actas 1: 82. Jujuy.

Cunningham, W.D. 1993. Strike-Slip Faults in the Southernmost Andes and the development of the Patagonian Orocline. Tectonics 12 (1): 169-186

Cunningham, W.D. 1995. Orogenesis at the southern tip of the Americas: the structural evolution of the Cordillera Darwin metamorphic complex, southernmost Chile. Tectonophysics 244: 197-229.

Cunningham, W.D.; Dalziel, I.W.D.; Lee, T.Y.; Lawver, L.A. 1995. Southernmost South America-Antarctic Peninsula relative plate motions since 84 Ma: implications for the tectonic evolution of the Scotia arc region. Journal of Geophysical Research 100 (B5): 8257-8266.

Dalziel, I.W.D.; De Wit, M.J.; Palmer, K.F. 1974. Fossil marginal basin in the southern Andes. Nature 250: 291-294.

Dalziel, I.W.D.; Palmer, K.F. 1979. Progressive deformation and orogenic uplift at the southern extremity of the Andes. Bulletin of the Geological Society America 90: 259-280.

Del Ventisette, C.; Montanari, D.; Sani, F.; Bonini, M. 2006. Basin inversion and fault reactivation in laboratory experiments. Journal of Structural Geology 28: 2067-2083.

Diraison, M.; Cobbold, P.R.; Gapais, D.; Rossello, E.A.; Gutiérrez Pleimling, A. 1997. Neogene tectonics within Magellan basin (Patagonia). *In* Simposio Bolivariano (Petroleum exploration in the Subandean basins), No. 6, Actas 1: 1-14. Cartagena de Indias.

Diraison, M.; Cobbold, P.R.; Gapais, D.; Rossello, E.A.; Le Corre, C. 2000. Cenozoic crustal thickening, wrenching and rifting in the foothills of the southernmost Andes. Tectonophysics 316: 91-119.

Dunlop, D.J.; Özdemir, Ö. 1997. Rock Magnetism: Fundamentals and Frontiers. Cambridge Studies. Cambridge University Press: 573 p. Cambridge.

Ghiglione, M.; Ramos, V. 2005. Progression of deformation and sedimentation in the southernmost Andes. Tectonophysics 405: 25-46.

Hanson, R.E.; Wilson, T.J. 1991. Submarine rhyolitic volcanism in a Jurassic proto-marginal basin, southern Andes, Chile and Argentina. *In* Andean magmatism and its tectonic setting (Harmon, R.S.; Rapela, C.W.; editors). Geological Society of America, Special Paper 265: 13-27.

Hrouda, F. 2002. Low-field variation of magnetic susceptibility and its effect on the anisotropy of magnetic susceptibility of rocks. Geophysical Journal International 150 (3): 715-723.

Jelinek, V. 1977. The statistical theory of measuring anisotropy of magnetic susceptibility of rock and its application. Geofyzika: 88 p.

Jelinek, V. 1978. Statistical processing of anisotropy of magnetic susceptibility measured on groups of specimens. Studia Geophyzika et Geodetika 22: 50-62.

Jelinek, V. 1981. Characterization of the magnetic fabric of rocks. Tectonophysics 79: T63-T67.

Katz, H.R. 1972. Plate tectonics and orogenic belts in the South-East Pacific. Nature 237: 331-332.

Klepeis, K.A. 1994. The Magallanes and Deseado fault zones: major segments of the South American-Scotia transform plate boundary in southernmost South America, Tierra del Fuego. Journal of Geophysical Research 99: 22001-22014.

Klepeis, K.A.; Austin Jr., J.A. 1997. Contrasting styles of superposed deformation in the southernmost Andes. Tectonics 16: 755-776.

Kraemer, P.E. 2003. Orogenic shortening and the origin of the Patagonian orocline (56°S.Lat.) Journal of South American Earth Sciences 15 (7): 731-748.

Kohn, M.J.; Spear, F.S.; Dalziel, I.W.D. 1993. Metamorphic PT paths from the Cordillera Darwin: a core complex in Tierra del Fuego, Chile. Journal of Petrology 34: 519-542.

Kohn, M.J.; Spear, F.S.; Harrison, T.M.; Dalziel, I.W.D. 1995. Ar^{40}/Ar^{39} geochronology and P-T-t paths from the Cordillera Darwin metamorphic complex, Tierra del Fuego, Chile. Journal of Metamorphic Geology 13: 251-270.

Letouzey, J. 1990. Fault reactivation, inversion and fold-thrust belt. *In* Petroleum and Tectonic in Mobile Belts (Letouzey, J.; editor). Technip: 101-128. Paris.

Lodolo, E.; Tassone, A.; Menichetti, M.; Lippai, H.; Hormaechea, J.L.; Ferrer, C.; Connon, G. 2001. The Magallanes-Fagnano Fault System in the Lago Fagnano, Tierra del Fuego Island: morphology and structure. *In* General Assembly of the European Geophysical Society (EGS), No. 26, Symposium Se. 5.02: 25-30. Nice.

Lodolo, E.; Menichetti, M.; Bartole, R.; Ben Avram, Z.; Tassone, A.; Lippai, H. 2003. Magallanes-Fagnano continental transform fault (Tierra del Fuego, southernmost South America). Tectonics 22 (6): 1076. DOI: 1029/2003TC0901500.

Martín-Hernández, F.; Dekkers, M.J.; Bominaar-Silkens, I.M.A.; Maan, J.C. 2008. Magnetic anisotropy behaviour of pyrrhotite as determined by low- and high-field experiments. Geophysical Journal

International 174 (1): 42-54. DOI: 10.1111/j.1365-246X.2008.03793.x

Menichetti, M.; Acevedo, R.D.; Bujalesky, G.G.; Cenni, M.; Cerredo, M.E.; Coronato, A.; Hormachea, J.L.; Lippai, H.; Lodolo, E.; Olivero, E.B.; Rabassa, J.; Tassone, A. 2004. Geology and geophysics of Isla Grande de Tierra del Fuego. Field-trip guide. Geosur: 39 p. Buenos Aires-Ushuaia.

Menichetti, M.; Lodolo, E.; Tassone, A. 2008. Structural geology of the Fuegian Andes and Magallanes fold-and-thrust belt-Tierra del Fuego Island. Geologica Acta 6 (1):19-42.

Nelson, E.P.; Dalziel, I.W.D.; Milnes, A.G. 1980. Structural geology of the Cordillera Darwin-collisional style orogenesis in the southernmost Chilean Andes. Eclogae Geologicae Helvetiae 73 (3): 727-751.

Olivero, E.B.; Malumián, D.R. 2008. Mesozoic-Cenozoic stratigraphy of the Fuegian Andes, Argentina. Geologica Acta 6 (1): 5-18.

Olivero, E.B.; Martinioni, D.R. 2001. A review of the geology of Argentinian Fuegian Andes. Journal of South American Earth Sciences 14: 175-188.

Olivero, E.B.; Martinioni, D.R.; Malumián, N.; Palamarczuk, S. 1999. Bosquejo geológico de la Isla Grande de Tierra del Fuego. *In* Congreso Geológico Argentino, No. 14, Actas 1: 291-294. Salta.

Olivero, E.B.; Medina, F.A.; López, M.I. 2009. The stratigraphy of Cretaceous mudstones in te eastern Fuegian Andes: New data from body and trace fossils. Revista de la Asociación Geológica Argentina 64 (1): 60-69.

Peroni, J.; Tassone, A.; Menichetti, M.; Lippai H.; Vilas, J.F. 2009. Geologia e geofisica del plutone del Cerro Trapecio-Tierra del Fuego-Argentina. Rendiconti Società Geologica Italiana, Nuova Serie 5: 160-163.

Petrovský, E.; Kapička, A. 2006. On determination of the Curie point from thermomagnetic curves. Journal of Geophysical Research 111 (B12S27), DOI: 10.1029/2006JB004507.

Rapalini, A.E.; Cerredo, M.E.; Tassone, A.; Lippai, H. 2005a. Estudio de magnetofábrica y microestructuras a través de los Andes de Tierra del Fuego. *In* Congreso Geológico Argentino, No. 16, Actas en CD: 8 p. La Plata.

Rapalini, A.E.; Lippai, H.; Tassone, A.; Cerredo, M.E. 2005b. An AMS and paleomagnetic study across the Andes in Tierra del Fuego. *In* International Symposium on Andean Geodynamics, No. 6, Actas: 596-599. Barcelona.

Suárez, M.; Pettigrew, T.H. 1976. An Upper Mesozoic island arc-back arc system in the southern Andes and South Georgia. Geological Magazine 113: 305-400.

Stern, C. 1980. Geochemistry of Chilean Ophiolites: Evidence for the compositional evolution of the mantle source of back-arc basin basalts. Journal of Geophysical Research 85 (2): 955-966.

Tarling, D.H.; Hrouda, F. 1993. The Magnetic Anisotropy of Rocks. Chapman and Hall: 217 p. London.

Wilson, T.J. 1991. Transition from back-arc to foreland basin development in the southernmost Andes: Stratigraphic record from the Última Esperanza District, Chile. Geological Society of America Bulletin 103: 98-111.

Zaffarana, C.B.; Somoza, R.; Olivero, E.B. 2008. Anisotropía de la susceptibilidad magnética en el Paleógeno de la faja plegada Fueguina. *In* Congreso Geológico Argentino, No. 17, Actas en CD: 168, Jujuy.

Manuscript received: January 9, 2009; revised/accepted: August 30, 2010.